# Multi-Megawatt-Scale Power-Hardware-in-the-Loop Interface for Testing Ancillary Grid Services by Converter-Coupled Generation

## Preprint

Przemyslaw Koralewicz, Vahan Gevorgian, and Robb Wallen
*National Renewable Energy Laboratory*

*Presented at the 18th IEEE Workshop on Control and Modeling for Power Electronics (COMPEL 2017)*
*Stanford, California*
*July 9–12, 2017*

**NREL is a national laboratory of the U.S. Department of Energy**
**Office of Energy Efficiency & Renewable Energy**
**Operated by the Alliance for Sustainable Energy, LLC**

This report is available at no cost from the National Renewable Energy Laboratory (NREL) at www.nrel.gov/publications.

**Conference Paper**
NREL/ CP-5D00-68856
July 2017

Contract No. DE-AC36-08GO28308

**NOTICE**



This report is available at no cost from the National Renewable Energy Laboratory (NREL) at www.nrel.gov/publications.

Available electronically at SciTech Connect http:/www.osti.gov/scitech

Available for a processing fee to U.S. Department of Energy and its contractors, in paper, from:

U.S. Department of Energy
Office of Scientific and Technical Information
P.O. Box 62
Oak Ridge, TN 37831-0062
OSTI http://www.osti.gov
Phone: 865.576.8401
Fax: 865.576.5728
Email: reports@osti.gov

Available for sale to the public, in paper, from:

U.S. Department of Commerce
National Technical Information Service
5301 Shawnee Road
Alexandra, VA 22312
NTIS http://www.ntis.gov
Phone: 800.553.6847 or 703.605.6000
Fax: 703.605.6900
Email: orders@ntis.gov

*Cover Photos by Dennis Schroeder: (left to right) NREL 26173, NREL 18302, NREL 19758, NREL 29642, NREL 19795.*

NREL prints on paper that contains recycled content.

# Multi-Megawatt-Scale Power-Hardware-in-the-Loop Interface for Testing Ancillary Grid Services by Converter-Coupled Generation


Przemyslaw Koralewicz
National Renewable Energy Laboratory
Golden, CO, USA
przemyslaw.koralewicz@nrel.gov

Vahan Gevorgian
National Renewable Energy Laboratory
Golden, CO, USA
vahan.gevorgian@nrel.gov

Robb Wallen
National Renewable Energy Laboratory
Golden, CO, USA
robb.wallen@nrel.gov



***Abstract*—Power-hardware-in-the-loop (PHIL) is a simulation tool that can support electrical systems engineers in the development and experimental validation of novel, advanced control schemes that ensure the robustness and resiliency of electrical grids that have high penetrations of low-inertia variable renewable resources. With PHIL, the impact of the device under test on a generation or distribution system can be analyzed using a real-time simulator (RTS). PHIL allows for the interconnection of the RTS with a 7 megavolt ampere (MVA) power amplifier to test multi-megawatt renewable assets available at the National Wind Technology Center (NWTC). This paper addresses issues related to the development of a PHIL interface that allows testing hardware devices at actual scale. In particular, the novel PHIL interface algorithm and high-speed digital interface, which minimize the critical loop delay, are discussed.**



***Keywords—Power grids; Microgrids; Power system reliability; Power system stability; Power system faults; Power quality; Wind energy integration; Test facilities; System testing***


## I. Introduction

With increasing penetration levels of low-inertia power electronic converters connected to the electric grid, it is crucial to deeply understand the interaction of these devices with the grid, including their impact on frequency and voltage regulation. Researchers use various methods to evaluate the impacts of different types of variable generation. For example, offline simulations can be detailed, but they often use simplified models of the device under test (DUT) and of the conditions in which it operates [1]. Another approach is to connect an actual DUT directly to a real grid; however, it is hard to verify all frequency and voltage event scenarios, and it may take a long time for the real events to happen. Alternatively, grid simulators are helpful because they allow replaying previously recorded or arbitrary patterns [2]. These testing capabilities work well provided that the grid has relatively small impedances and that the power fed by the DUT back to the grid does not impact the voltage or frequency of the system. When that happens, PHIL provides a solution, allowing for the seamless integration of physical power generators with software models in a single, closed-loop simulation. The grid is modeled in the RTS, and the voltage at its terminals is replicated using a power amplifier on the terminals of the DUT; the DUT is then able to sense the grid frequency and voltage and operate as if it were connected to the simulated grid. Power generated by the DUT is measured by the RTS and fed back in real time to a simulated model, allowing for the analysis of its impact on the grid. This functionality is essential to analyzing grids or microgrids that are characterized by high penetration levels of low-inertia power electronics converters and studying the impact of the ancillary services, which are provided by many devices to support the grid in case of various events.

This paper describes the PHIL interface developed at the NWTC which allows coupling a Real Time Digital Simulator (RTDS) RTS to various utility-scale renewable generation assets, including multiple wind turbines ranging from 0.5–3 MW; a 1-MW battery energy storage system; a 0.5-MW solar installation; and various equipment that can be tested at the site on a temporary basis, including fuel cells and microgrid controllers.

## II. Power and Control Hardware

A typical PHIL experiment setup is shown in Fig. 1. The power side consists of various DUTs and a 7-MVA controllable grid interface (CGI) acting as a low-latency controllable voltage source. Fig. 1 shows a 1.5-MW wind turbine with a commercial wind power plant controller and the embedded capability to provide ancillary services. The RTDS RTS is capable of the real-time execution of the generation and distribution models with a typical time step of 50 $\mu s$. A detailed description of the model used to conduct the tests

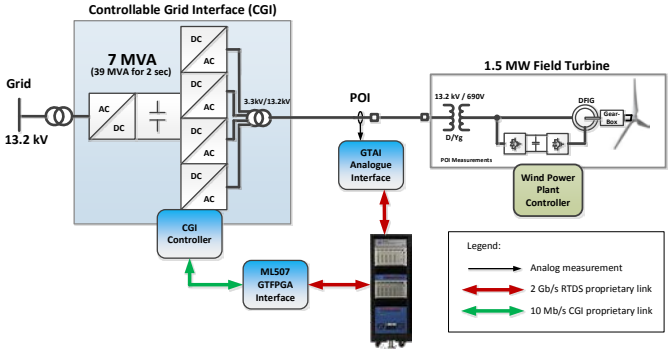


Fig. 1. Example PHIL setup with CGI, RTDS, and a 1.5-MW wind turbine

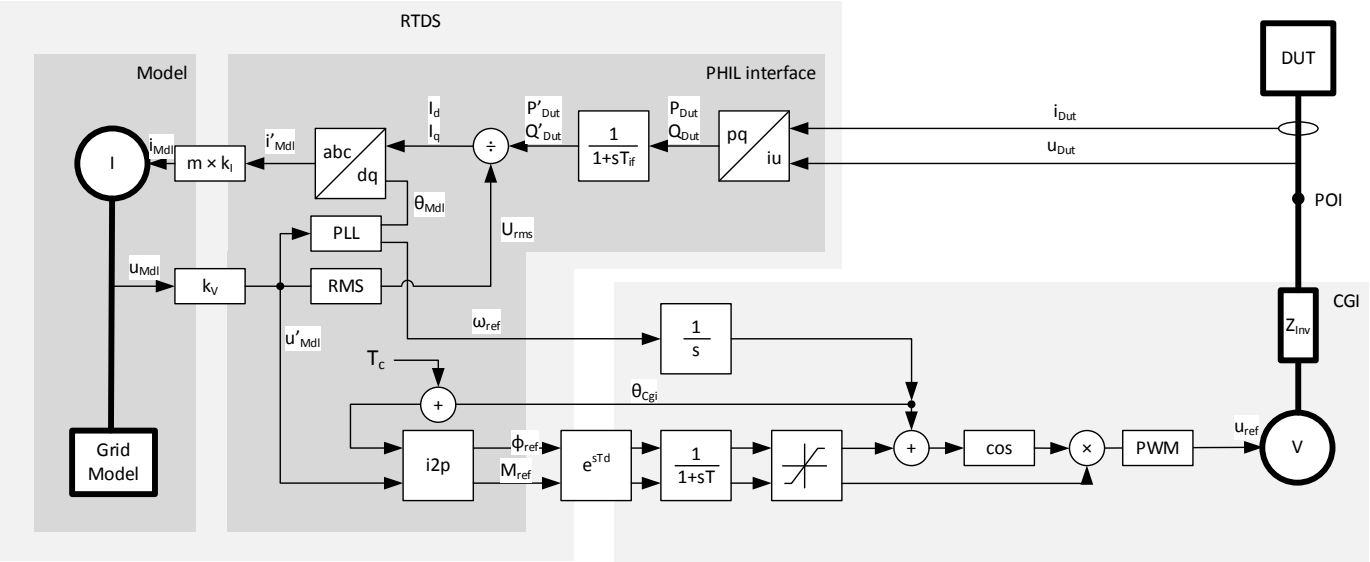


Fig. 2. Block diagram of the PHIL interface

described in this paper is given in Section V. The voltage at a single node of the simulated model is monitored and commanded to the CGI. At the same time, the current at the point of interconnection (POI) is measured using Rogowski coils and fed back to the RTDS.

Because of the large footprint of the test setup, a dedicated fiber-optic network communication system was implemented to exchange measurements and set points among the CGI, DUT, and RTDS using the minimum latency required by the closed-loop systems instead of traditional analog signal interfaces [4-6]. The DUT voltage, $u_{Dut}$, and current, $i_{Dut}$, waveforms are measured with a standard RTDS analog input card located near the DUT's POI, which is far from the main RTDS rack. Voltages and currents are collected with a high sampling rate of 25 µs, digitally filtered for antialiasing effects, and transmitted back to the central RTDS unit using a 2 Gb/s fiber optic channel, thus reducing the latency of the measurement to less than 10 µs. At the same time, the voltage commands from the RTDS are transmitted after every 50 µs time step by utilizing the 2 Gb/s optical link to the ML507 Xilinx evaluation board, which acts as a protocol translator allowing an interface with the CGI by using proprietary optical protocol and making it possible to deterministically exchange 20 x 16-bit words every 25 µs.

## III. Modeling the PHIL Interface

The PHIL interface is a coupler between a model of the grid implemented in the RTDS and a real DUT in the field. The block diagram is shown in Fig. 2. The PHIL's basic principle is that voltage measured at the simulated model's single bus is replicated at the real system's bus using grid simulation. Simultaneously, the current flowing into the grid simulator is measured and injected back into the simulated model. Model and real-world per-unit (p.u.) systems may differ, so voltage-scaling, $k_V$, and current-scaling, $k_I$, factors are used. Additionally, the impact of the DUT on the grid model can be adjusted by manipulating the multiplication factor $m$. In the case of $m = 0$, the test is called an open loop, and allows the DUT to "see" the voltage of the modeled grid, but no feedback is enabled. Increasing the $m$ factor multiplies the impact of power flowing from the DUT on the modeled grid, which thus allows for testing variables such as the penetration levels of renewable energy on a given grid.

The main objectives of the NWTC's PHIL interface implementation are as follows:

- Accurate, low-latency, instantaneous voltage tracking of the modeled voltage, $u'_{Mdl}$, by actual CGI voltage, $u_{ref}$
- Accurate tracking of positive, negative, and zero sequence components of modelled voltage $u'_{Mdl}$, by actual CGI voltage,
- Accurate tracking of actual DUT active and reactive power(measured using $i_{Dut}$ and $u_{Dut}$) in the model.

Fulfilling the above objectives allows for multiple tests validating the DUT's ancillary services, including frequency response, voltage regulation, and volt/volt-ampere reactive (VAR) support.

Voltage tracking by the CGI is complicated by the fact that the CGI is intended to operate using phasor set points rather than instantaneous set points, whereas it is desired to implement an instantaneous model in the RTS. An instantaneous-to-phasor (I2P) algorithm is therefore developed to convert the modeled instantaneous voltages $u'_{Mdl}$ into phasor magnitudes, $M_{ref}$, and angle set points, $\phi_{ref}$, for each phase independently so that the CGI's instantaneous voltage $u_{ref}$ is able to track the modeled voltages in terms of phase, magnitude, and frequency both in steady state and during transient. Section IV further describes the I2P algorithm's design and performance validation.

Power tracking in the real-time model is implemented using active and reactive power measurements taken at the POI. These are then filtered to ensure the stability of the closed-loop

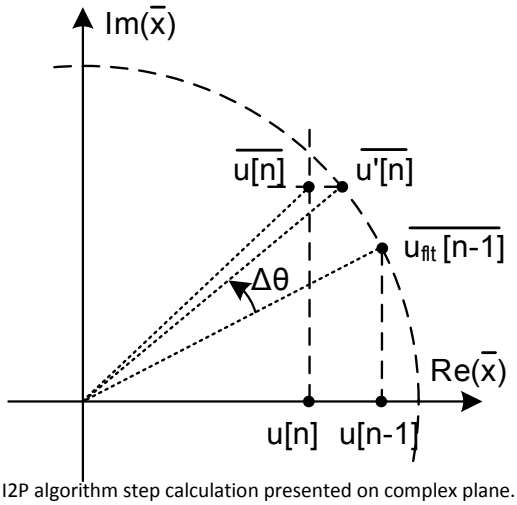


Fig. 3. I2P algorithm step calculation presented on complex plane.

PHIL experiment and they are divided by the voltage, $U_{rms}$, to extract the $I_d$ and $I_q$ components of the current. The angle of the modeled voltage, $\theta_{Mdl}$, is reconstructed using a phase-locked loop and used to synthesize the instantaneous current references, $i_{Mdl}$, which control the current sources in the grid model.

## IV. Single Phase Instantaneous to Phasor Algorithm

As an electromagnetic transient model program, most of the variables observed within an RTDS simulation model correspond to instantaneous values of voltage and current. Since CGI only accepts polar phasor references, an algorithm had to be developed to allow for real-time conversion. Due to the requirement of accurately tracking positive, negative and zero sequence voltages and the fact that CGI inputs are independent single phase phasors, it was desired to implement the I2P algorithm as a single phase module. Three identical blocks are then used to implement the three-phase PHIL algorithm.The block design is described in this chapter. Fig. 3 shows the voltage vector rotating on a complex plane and the principles of smooth optimization. Fig. 4 shows a block diagram of calculations done in the I2P algorithm

Since the I2P algorithm needs to be implemented in real-time environment with calculations executed in constant time step a discrete equations are used. Calculating the actual step outputs $M$[n] and $\phi[n]$ is based on actual inputs $u[n]$ and $\theta[n]$, and the previous state of the rotating phasor vector, $\overline{u_{flt}[n-1]}$.

The algorithm's main objective is to calculate the magnitude, $M$[n], and angle, $\varphi[n]$, that will be sent to CGI based on the instantaneous value of voltage in any given phase, $u[n]$, and the actual angle of the CGI's integrator, $\theta[n]$. CGI modulator rotates the phasor using the cosine function, thus, as long as formula (1) is met, then the actual instantaneous voltage at the output of the modulator will be equal to the instantaneous input voltage.

$$u[n] = M[n]cos(\Phi[n] + \theta[n]) \tag{1}$$

Since two variables need to be calculated and only one equation satisfies the main objective, it means that there is one degree of freedom which can be used to satisfy the secondary objective of a smooth phasor reference to the CGI, both in steady state and during transitions.. Point $\overline{u_{flt}[n-1]}$ corresponds to an actual phasor reference sent to the CGI in previous a cycle, $\overline{U_{flt}[n-1]}$, rotated by the integrator angle from a previous calculation step, $[n-1]$ , as shown in (2).

$$\overline{u_{flt}[n-1]} = \overline{U_{flt}[n-1]}e^{i\theta[n-1]} \tag{2}$$

Projection of this point on a real axis corresponds to the actual instantaneous output voltage at previous step $u[n-1]$.

Based on the previous phasor reference, a $\overline{u'[n]}$ point coordinates are calculated by rotating the actual CGI's reference from the previous step by the actual integrator angle, $\theta[n]$.

$$\overline{u'[n]} = \overline{U_{flt}[n-1]}e^{i\theta[n]} \tag{3}$$

Thus, this point can be interpreted as the first estimate of the $\overline{u[n]}$ point assuming that the input voltage phasor is oscillating steadily with nominal frequency and equals to $\overline{U_{flt}[n-1]}$. Essentially, when (4) is met, $\overline{u'[n]}$ becomes $\overline{u[n]}$.

$$\overline{U_{flt}[n-1]} = \overline{U_{flt}[n]} \tag{4}$$

However, this assumption is not always met in the dynamic system, so the algorithm needs to be able to respond to transients and lack of synchronization issues. To address that

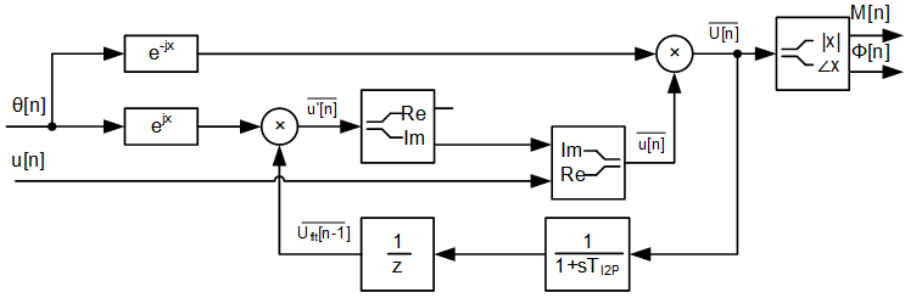


Fig. 4. Block diagram showing calculations within I2P algorithm

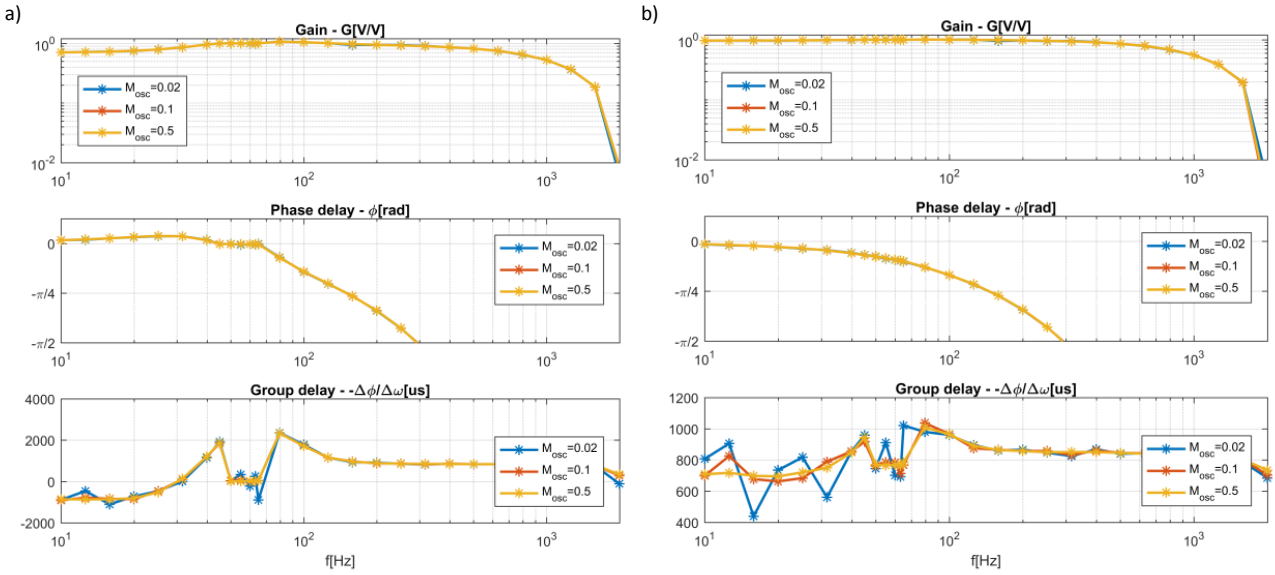


Fig. 5. Voltage tracking path transfer funtion analysis. a) without delay compensation b) with delay compensation using$T_C$

$\overline{u[n]}$ point is built as shown in (5).

$$\overline{u[n]} = u[n] + i\, Im\{\overline{u'[n]}\} \tag{5}$$

Equation (5) ensures that the actual instantaneous voltage at the output of modulator is equal to the instantaneous input by setting the real part to $u[n]$. The imaginary part of the point is selected so that $\overline{u[n]}$ is closest to the estimated point $\overline{u'[n]}$. This is always achieved when their imaginary parts are equal. A new point calculated in the rotating plane must be reverted back to the stationary frame before sending the reference to the CGI,

$$\overline{U[n]} = \overline{u[n]}e^{-i\theta[n]}. \tag{6}$$

Since the CGI uses polar coordinates as references, they must be converted to $M$[n] and $\phi[n]$ before sending.

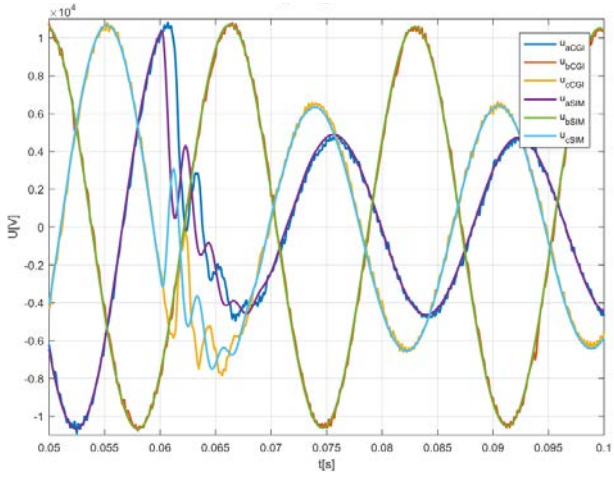


Fig. 6. Voltage fault tracking through the PHIL interface without delay compensation

The real and reactive part of actual phasor values are filtered through a single pole, low-pass filter to assure that a steady state is always achieved for voltages oscillating with nominal frequency and steady magnitude and angle. Then, a single cycle delay is applied to avoid an algebraic loop before this point is used for the next cycle calculations.

### *A. Transfer function analysis and delay compensation*

The design of the I2P algorithm shown in Section IV is idealized and assumes no delays between the RTDS and the CGI. However, various delays do exist in the system due to communications and processing times. These delays are summarized and visualized in Fig. 2 as the $e^{sT_d}$ block. If no delay compensation technique is used, then the voltage tracking will be optimized to reproduce the voltage's fundamental component with the highest precision and minimum delay between the simulated and actual voltage, while other frequency components will show various delays. The system transfer function was analyzed using a detailed Simulink model of the system, which included all the delays and a modulator model. Small signal oscillation sweeping through frequency range from 10Hz to 2kHz was generated as voltage at modeled RTDS side, $u_{Mdl}$ Simultaneously, the given frequency was measured at the modulator's output, $u_{ref}$ . Fig. 5a shows the Bode plot of this transfer function. For frequencies at the CGI's nominal operating range, 45–65 Hz of magnitude, the gain ($G$) is close to 1.0 and phase shift ($\phi$) is close to 0 radians, which indicates good synchronization of the fundamental frequency signal. Below the nominal operating range, the frequency phase shift is slightly positive, indicating that output voltage slightly leads against the model. Above the nominal operating range, the frequency phase shift veers negative—thus, the output voltage is slightly delayed compared to the input voltage. The last plot shows group delay calculated as a phase shift derivative with respect to frequency. A flat group delay plot versus frequency indicates fewer

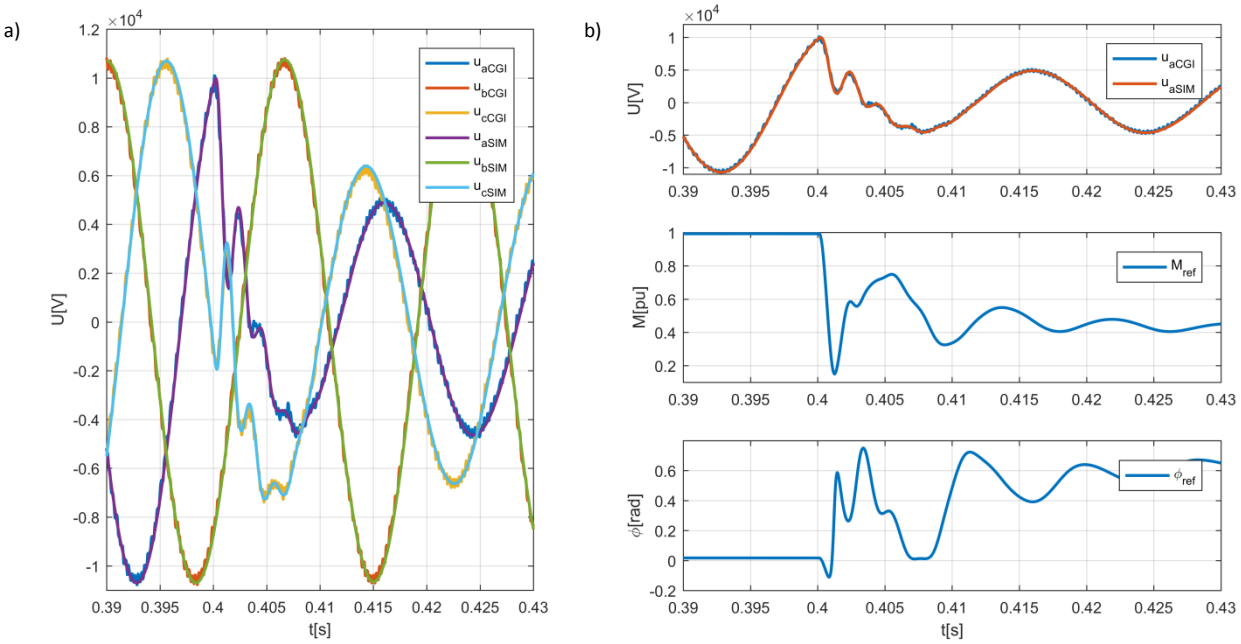


Fig. 7. Single phase line to line fault example. a) voltage tracking during transition, b) CGI voltage reference of phase A during the fault event

distortions have been added to the output signal because more frequencies are delayed by exactly the same amount of time. With no delay compensation, the plot shows significant variability with values ranging between -800 us and 2000 us, which indicatesthat distortions may be significant in wide-frequency spectrum signals.

Fig. 6 shows the PHIL interface's voltage tracking capabilities for wide-frequency spectrum voltage signals–a single line to line voltage fault. Before the event at t=0.06s, voltage tracking is excellent–the CGI and the simulated voltages are synced. A step change in modeled voltage is observed during the fault. Due to the wide-frequency spectrum of this kind of signal, the voltage distortion is visible. After t=0.075s, the voltage reaches steady state and, much like the period before the event, synchronization can once again be observed.

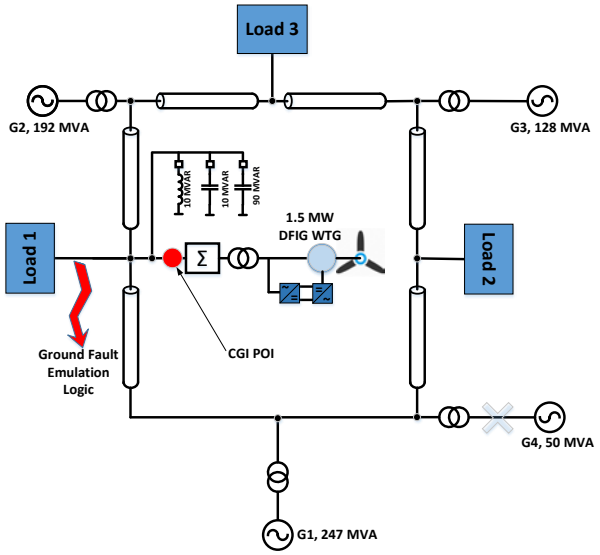


Fig. 8. Overview of the 9-bus model

Fig. 5b shows the same transfer function after applying a delay compensation, $T_c$, which is equal in value to the sum of all system delays, $T_d$, to the angle signal feed to the RTDS from the CGI's integrator, $\theta_{cgi}$. The delay compensation changed the phase delay profile. Now, it decreases steadily with frequency and is always negative. The output voltage is delayed when compared to the simulation. The group delay also shows a substantial difference, and a flatter plot is observed. An example of a wide-spectrum signal passing through the PHIL interface is shown in Fig. 7a. There are negligible voltage tracking errors during steady state and transition, indicating the delay compensation was correctly added. The measured CGI's output voltage signal was shifted in time by $T_d$ to allow a better comparison of the delayed signal distortions. Additionally, Fig. 7b shows that in the steady state before the event, both magnitude and phase are smooth, thus indicating that the CGI's optimal operation has been achieved. During the transient reference voltage, the vector changes dynamically. However, the rate of change is not fast enough to cause disturbances due to the CGI's limitations. The delay compensation drawback is that output signals are delayed compared to simulated signals, thus limiting the maximum bandwidth of simulation that can be achieved in a PHIL type of experiment.

## V. Grid Modelling

The model of the 130-kV transmission grid used for the experiment, shown in Fig. 8, consists of four generators with a total capacity of 617 MW [3]. During the experiment, the steady-state total system load is 400 MW. An automatic generation control (AGC) has been implemented to control overall system frequency. The model allowed multiple types of

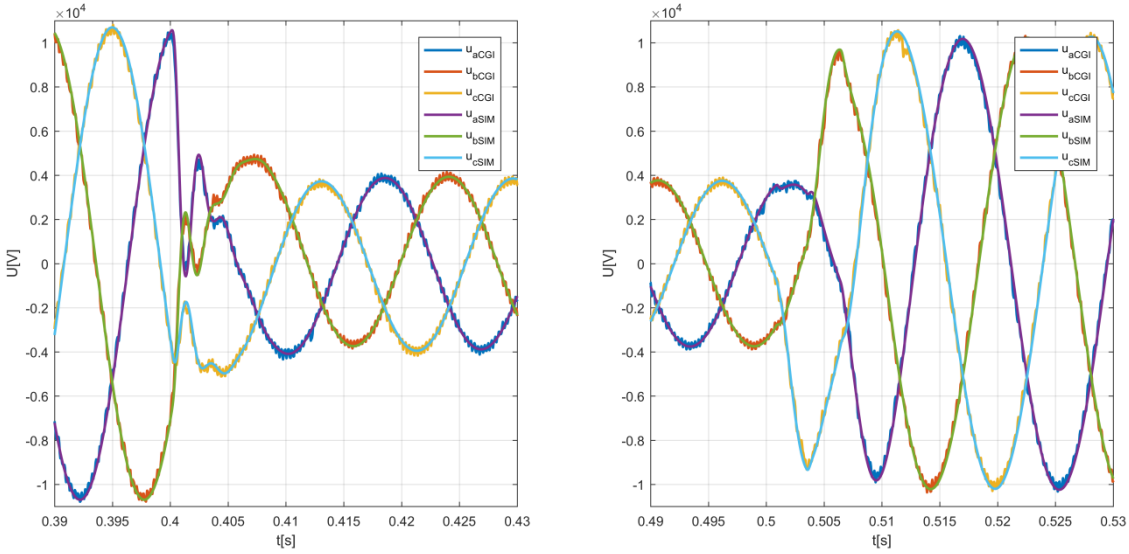


Fig. 9. Three phase line to ground test

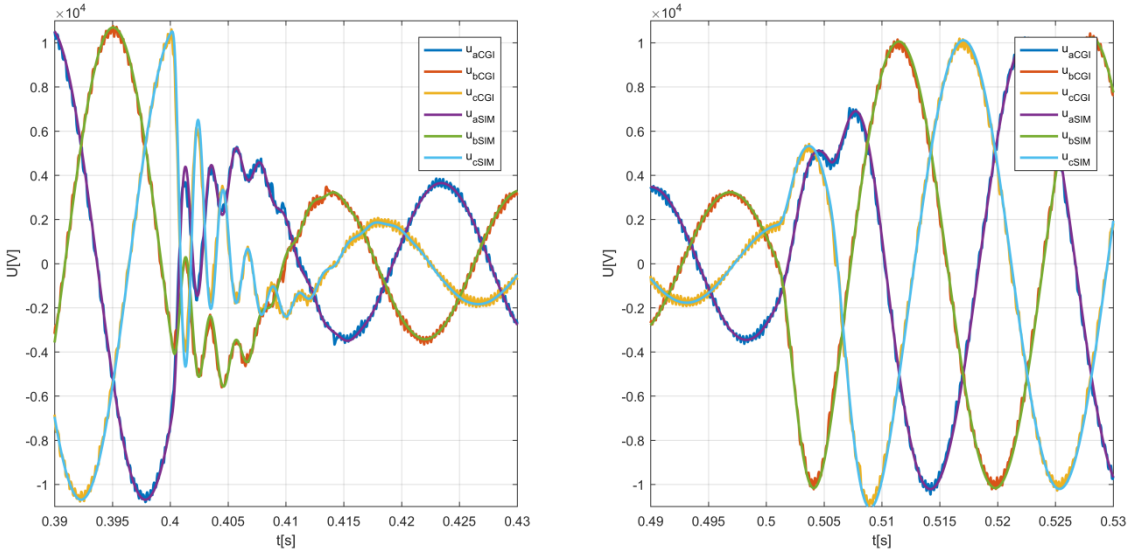


Fig. 10. Two phase line to line fault

tests that show the interaction between transmission system and device under test.

## VI. Experimental Results

### A. Fault testing

Various types of faults can happen in a power grid. The PHIL interface allows evaluation of an impact of the fault simulated in one of busses of the model on real DUT. Various ride-through techniques can be tested. At the same time, the DUT's grid-supporting features, such as injecting a reactive current, can be tested. Verifying these features usually requires an open-loop approach, however, the PHIL interface verifies the efficiency of such scheme at a system level.

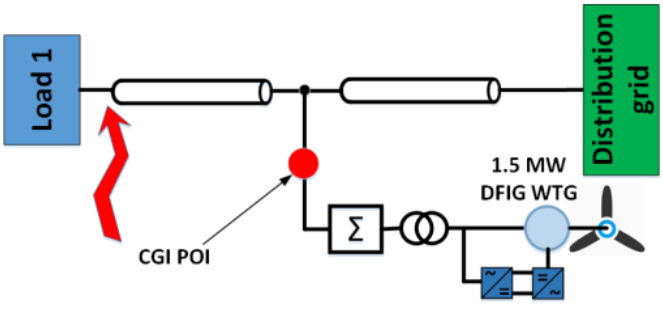


Fig. 11. Fault testing circuit

Fig. 11 shows a testing circuit embedded in the RTDS model that was used for evaluating various fault scenarios. A fault was located at load 1 bus, which is connected to the main transmission grid ring through impedance $Z_L$. The POI for the PHIL test was located at 20% of the line length from Load 1, thus the fault was effectively happening behind 0.2 $Z_L$ impedance, as seen from the DUT perspective.

Both line-to-line and line-to-ground tests have been conducted to validate the PHIL interface's capability to track fast-changing and highly asymmetric voltages during such faults. Some of them are shown in this paper, including single-phase line-to-line tests in Fig. 7, two-phase line-to-line faults in Fig. 10, and three-phase line-to-ground tests in Fig. 9. All of these tests show the superior tracking capabilities of the PHIL interface. Apart from step change, which is precisely emulated, PHIL can also track oscillation with circa 400Hz characteristic frequency of modelled circuit that happens after the step change and is typically damped within 10–20 ms due to the high bandwidth of the PHIL interface and the CGI.

### *B. Frequency response testing*

TABLE I. GENERATOR LOSS FREQUENCY DIP SUMMARY

| m | $f_{min}$ [Hz] |
|---|---|
| 0 | 59.606 |
| 3 | 59.608 |
| 60 | 59.621 |
| 100 | 59.625 |

Multiple tests were conducted to show the impact of a generator loss contingency event on grid frequency, and selected results are shown in TABLE I. Prior to the contingency emulation, the wind turbine was set to operate in curtailed mode with maximum power at 1 MW, thus allowing 0.5 MW of headroom for regulation purposes. At $t = 0.9\ s$, a circuit breaker from Generator 4 was commanded to open, causing the instantaneous loss of 50 MW

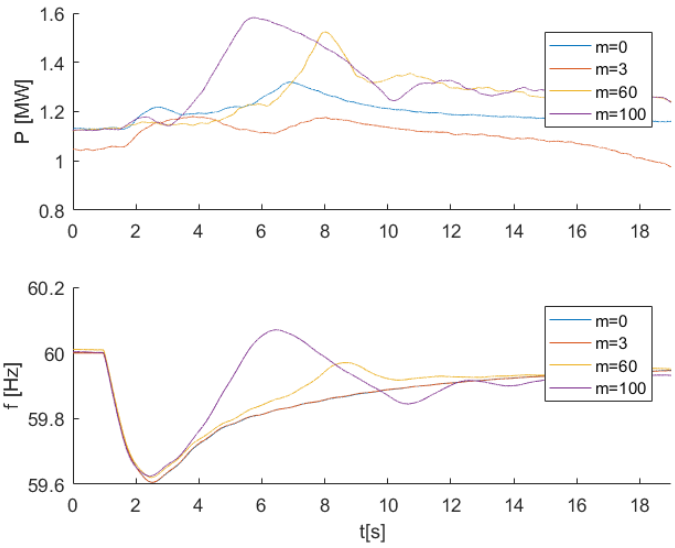


Fig. 12. Frequency response testing

of generation out of 450 MW of total generation. The system frequency declines to 59.606 Hz and then slowly recovers due to a combination of primary frequency control and AGC implemented in the RTDS model. (Note that it is important to limit the depth of the frequency event because it can cause various grid protective devices to trip an entire system). The wind turbine supports the grid by injecting additional active power to the grid during the under-frequency event by using synthetic inertia and Hz/kW droop curves. All four events in Fig. 12 show the inertial response of the turbine, which increases the turbine's active power by approximately 100 kW within 1 s starting after the frequency fell to less than 59.8 Hz. This aligns with the DUT configuration. The droop starts to operate later because it is implemented in the wind power plant controller instead of the turbine's inertial controller. For comparison, see the case when $m = 0$ shows the system's frequency response without the PHIL feedback. At $m = 3$,

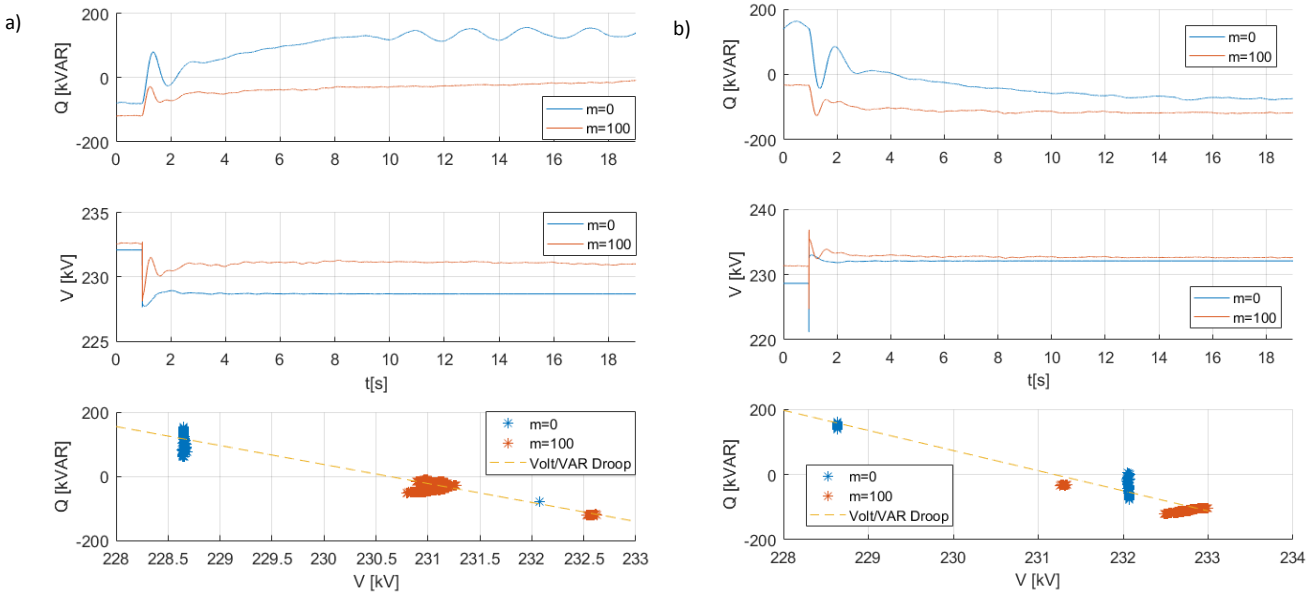


Fig. 13. A wind power plant's voltage regulator response to a capacitor bank: a) disabling event, b) enabling event

nearly no impact on system frequency can be observed because the inertial response of 3 x 100 kW is negligible compared to a 50-MW loss. At m = 60 and m = 100, the impact of the turbine's grid support is visible because its inertial response translates to 6 MW and 10 MW, respectively, of additional generation, thus helping to reduce the frequency dip to 59.621 Hz and 59.625 Hz. The PHIL experiment also demonstrates how AGC interacts with the droop response by causing a slight oscillation and overshoot of the frequency that needs to be damped.

### C. *Wind power plant control voltage testing*

Another useful case for a PHIL experiment is voltage control verification and its impact on grid stability and operation. In this case, a wind power plant controller operates with a volt/VAR droop that is intended to support the grid with voltage control by injecting reactive power into the system. Fig. 13 shows the response of a wind power plant to a step in the system voltage caused by the 10-MVAR capacitor bank connection and disconnection. Without the wind turbine's support, the turbine injects reactive power at $m = 0$ according to the droop curve marked with the dotted line on the bottom subplot. Because the impact to the grid is not modeled, additional reactive current does not help correct the voltage and thus the turbine operates at a different set point than it was when the feedback was enabled: $m = 100$ . The PHIL experiment also allows for studying the dynamic response of the voltage controller and its interaction with the grid impedance, which in some cases could lead to power oscillations and which would not be captured if only an open-loop system were analyzed. For example, an overshoot just after an event might be assumed, which in this case would be very well damped.

## VII. Conclusions

The PHIL system developed at the NWTC is a breakthrough in utility-scale grid integration testing capability that allows for studies of system stability, including detailed models of generation and distribution combined with real distributed-power assets that are already installed at the NWTC and testing devices that can be installed at the NWTC on a temporary basis. Results shown confirm the system's performance and allow for further studies of systems that are highly penetrated by low-inertia distributed resources with power electronics. This paper shows high flexibility and improved system performance of the system that can be used for multiple type of tests, from testing high-bandwidth fault events to evaluating long-term algorithms through various type of closed-loop, grid-connected inverters with features like droop or inertia . PHIL testing of newly commissioned systems shall be considered an intermediate step between offline modeling and final commissioning of many complex systems such as microgrids.

## Acknowledgment

This work was supported by DOE under Contract No. DE-AC36-08GO28308 with NREL. Funding provided by U.S. DOE Office of Energy Efficiency and Renewable Energy Wind Program. The authors would also like to thank Mr. Charlton Clark and Dr. Jian Fu of the U.S. DOE Wind Energy Technologies Office for their continuous support of research under this project. The authors would also like the ABB MV Drives Division in Turgi, Switzerland for their support of this work.

## References

[1] P. Kotsampopoulos, N. Hatziafyrion, B. Bletterie, G. lauss, T. Strausser, "Introdution of advanced testing procedures including PHIL for DG providing ancillary services," IECON 2013 conference paper, Nov 10-13, 2013

[2] P. Koralewicz, V. Gevorgian, R. Wallen, W. van der Merwe, P. Jörg, "Advanced Grid Simulator for Multi-Megawatt Power Converter Testing and Certification," IEEE Transactions on Energy Conversion, ECCE 2016 conference

[3] V. Gevorgian, P. Koralewicz, R. Wallen, E. Muljadi, X. Wang, "Controllable Grid Interface for Testing Ancillary Service Controls and Fault Performance of Utility-Scale Wind Power Generation," 15th International Workshop on Large-Scale Integration of Wind Power into Power Systems as well as on Transmission Networks for Offshore Wind Power

[4] W. Ren, M. Steurer, T.L. Baldwin, "Improve the Stability and the Accuracy of Power Hardware-in-the-Loop Simulation by Selecting Appropriate Interface Algorithms," IEEE Transactions on Industry Applications (44:4); pp. 1286–1294, 2008.

[5] N. Ainsworth, A. Hariri, K. Prabakar, A. Pratt, M. Baggu, "Modeling and Compensation Design for a Power Hardware-in-the-Loop Simulation of an AC Distribution System", North American Power Symposium (NAPS), pp. 1-6, 20106

[6] F. Huerta, R.L. Tello, M. Prodanovic, "Real-Time Power Hardware-In-The-Loop Implementation of Variable-Speed Wind Turbines", IEEE Transactions on Industrial Electronics; pp. 1893-1904, 2017